A NONLINEAR MODEL FOR FLUID-COUPLED VIBRATIONS OF SPENT NUCLEAR RACKS

Miguel Moreira
Mathematical Department, College of Technology, Setúbal Polytechnic , Portugal
José Antunes
Applied Dynamics Laboratory, ITN, Lisbon, Portugal

ABSTRACT

In the near-past we introduced a simplified linearized model for the fluid-coupled vibratory responses of nuclear fuel racks, neglecting three-dimensional flow effects and assuming small gaps between the fuel assemblies. In this paper, using the same basic approach, we generalize the above-mentioned model to account for nonlinear squeeze-film and dissipative flow effects. The proposed methodology can be automatically implemented on a symbolic computer environment. Numerical simulations highlight the significance of nonlinear flow effects at high vibration amplitudes, yielding more realistic predictions.

1. INTRODUCTION

Spent fuel storage racks are welded honeycomb stainless steel structures (generally described as blocks with rectangular walls) with large surfaces (the area of a rack wall can be of the order of 10 m^2). They are used to accommodate spent nuclear fuel assemblies. The spent fuel racks are placed on a fuel pool freely on the floor and are separated by small water gaps (sometimes down to the order of 10 mm). The fuel pool is filled with water several meters above the top of the racks. Fluid effects induce strong coupling between immersed nuclear fuel racks, when they are subjected to earthquake excitations [see for instance Broc et al (2000); Stabel and Ren (2001); Zhao et al (1996); Hinderks et al (2001)]. Therefore, during a seismic event, spent fuel storage racks may bend, slide, twist and uplift. Note that, racks are designed with short aspect ratios so that they would not tilt over. Undoubted understanding the complex dynamic behaviour of immersed spent fuel assemblies storage racks under earthquake is of prime importance for the safety of nuclear plant facilities.

In the near-past [Moreira and Antunes (2002)] we introduced a simplified linearized model for the fluid-coupled vibratory responses of nuclear fuel racks based on the following main simplifying assumptions: (i) Three-dimensional flow effects were neglected; (ii) Gaps between the fuel assemblies and between these and the container were small when compared with the longitudinal length-scales; (iii) Dynamical fluid effects were linearized. From these assumptions, we postulated a simplified flow inside the channels, such that the gap-averaged velocity and pressure fields were described in terms of a single space- coordinate, for each fluid channel. Time-domain simulations of the system responses to seismic excitations were also produced and, despite the simplifications introduced, the model yielded qualitatively similar predictions when compared with other recently published work. However, nonlinear squeeze-film and dissipative effects connected with very large amplitude responses cannot be properly modeled unless assumption (iii) is relaxed. Such is the aim of the present paper. Here, using the same basic approach, we generalize the above-mentioned model to account for nonlinear flow effects. Although algebraically involved, the proposed methodology can be automatically implemented on a symbolic computer environment, leading to a system of DAE's which is then solved through adequate time-step integration solver.

2. MODEL FORMULATION

2.1. Fluid Formulation

Consider a pool with $M \times N$ nuclear spent fuel racks arranged in M lines and N columns, which will be described using matrix notation.

The dimensions along the principal directions of each rack cross-section are L_X and L_Y. The X- and Y-direction channels (between each pair of racks or between a wall and a rack) are denoted as

$$H_j^X \,,\ 1 \ \leq \ i \leq M+1, \tag{1}$$

$$H_j^Y \,,\ 1 \ \leq \ j \leq N+1. \tag{2}$$

In Figure 1 one can see the main geometrical parameters, for a quite general system configuration.

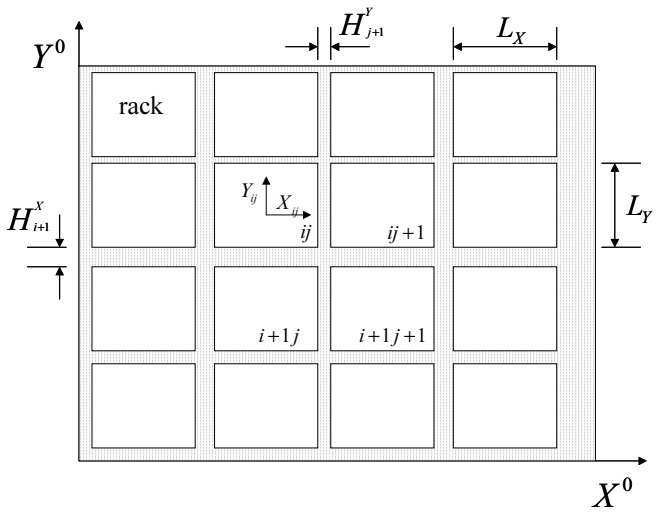

Figure 1: *Main geometrical parameters.*

The absolute positions of each rack $\left(\tilde{X}_{ij}(t), \tilde{Y}_{ij}(t)\right)$ can be defined as

$$\tilde{X}_{ij}(t) = X^0_{ij} + X_{ij}(t), \quad (3)$$

$$\tilde{Y}_{ij}(t) = Y^0_{ij} + Y_{ij}(t), \quad (4)$$

where $\left(X^0_{ij}, Y^0_{ij}\right)$ are the coordinates of the geometric centers with respect to the pool container, that is, $(X_{ij}(t), Y_{ij}(t))$ are the local coordinates of each rack. So, the actual X-direction $h^X$and Y-direction gaps h^Y can be defined as

$$h^X_{ij} = H^X_i + Y_{i-1j} - Y_{ij}, \left\{ \begin{array}{l} 1 \le i \le M+1 \\ 1 \le j \le N \end{array} \right. \quad (5)$$

and

$$h^Y_{ij} = H^Y_j + X_{ij} - X_{ij-1}, \left\{ \begin{array}{l} 1 \le i \le M \\ 1 \le j \le N+1 \end{array} \right. \quad (6)$$

where

$$Y_{0j} = Y_{M+1j} = X_{i0} = X_{iN+1} = 0$$

by definition. Note also that

$$\dot{h}^X_{ij} = \dot{Y}_{i-1j} - \dot{Y}_{ij}, \left\{ \begin{array}{l} 1 \le i \le M+1 \\ 1 \le j \le N \end{array} \right. , \quad (7)$$

$$\dot{h}^Y_{ij} = \dot{X}_{ij} - \dot{X}_{ij-1}, \left\{ \begin{array}{l} 1 \le i \le M \\ 1 \le j \le N+1 \end{array} \right. \quad (8)$$

and

$$\ddot{h}^X_{ij} = \ddot{Y}_{i-1j} - \ddot{Y}_{ij}, \left\{ \begin{array}{l} 1 \le i \le M+1 \\ 1 \le j \le N \end{array} \right. , \quad (9)$$

$$\ddot{h}^Y_{ij} = \ddot{X}_{ij} - \ddot{X}_{ij-1}, \left\{ \begin{array}{l} 1 \le i \le M \\ 1 \le j \le N+1 \end{array} \right. . \quad (10)$$

Following Antunes and Piteau (2000), a simplified flow model inside the X-direction and Y-direction channels can be developed from the abovementionned assumptions. With this approach the gap-averaged velocity and the pressure fields are described in terms of a single space coordinate and the continuity and momentum equations, in each channel, can be formulated as

$$\frac{\partial h}{\partial t} + \frac{\partial}{\partial z}(uh) = 0 \quad (11)$$

and

$$\rho\left[\frac{\partial}{\partial t}(uh) + h\frac{\partial}{\partial z}\left(u^2\right)\right] + \rho u|u| f + h\frac{\partial p}{\partial z} = 0 \quad (12)$$

where $u = u(z,t)$, $h = h(t)$, $p = p(z,t)$ and z stand respectively for the fluid velocity, channel gap, pressure and single spatial coordinate along the channel length. The parameter f represents an appropriate skin-friction coefficient accounting for the flow/walls distributed stresses. Typically f changes with the flow Reynolds number as $f = a\mathrm{Re}^b$ for adequate parameters a and b [see, for instance Hirs (1973)].

Integration of the continuity equation (11), leads to the general velocity field for the X-direction and Y-direction channels as

$$u^X_{ij}(x,t) = -\frac{\dot{h}^X_{ij}}{h^X_{ij}}x + C^X_{ij}, \quad (13)$$

with $1 \le i \le M+1$, $1 \le j \le N$, and

$$u^Y_{ij}(y,t) = -\frac{\dot{h}^Y_{ij}}{h^Y_{ij}}y + C^Y_{ij}, \quad (14)$$

with $1 \le i \le M$ and $1 \le j \le N+1$, where C^X_{ij} and C^Y_{ij} are functions of time stemming from the integration.

The following forms of equation (12) can be deduced for the X-direction (with $1 \le i \le M+1$ and $1 \le j \le N$) and Y-direction channels (with $1 \le i \le M$ and $1 \le j \le N+1$)

$$\frac{\partial p^X_{ij}}{\partial x} = -\rho \left\{ \begin{array}{l} \frac{1}{h^X_{ij}}\frac{\partial}{\partial t}\left(u^X_{ij}h^X_{ij}\right) \\ +2u^X_{ij}\frac{\partial}{\partial x}\left(u^X_{ij}\right) \\ +\frac{1}{h^X_{ij}}u^X_{ij}\left|u^X_{ij}\right| f \end{array} \right\}, \quad (15)$$

$$\frac{\partial p^Y_{ij}}{\partial y} = -\rho \left\{ \begin{array}{l} \frac{1}{h^Y_{ij}}\frac{\partial}{\partial t}\left(u^Y_{ij}h^Y_{ij}\right) \\ +2u^Y_{ij}\frac{\partial}{\partial y}\left(u^Y_{ij}\right) \\ +\frac{1}{h^Y_{ij}}u^Y_{ij}\left|u^Y_{ij}\right| f \end{array} \right\}, \quad (16)$$

where p_{ij}^X and p_{ij}^Y are the pressures along X-direction and Y-direction channels.

Integration of equations (15)-(16) yields for $1 \leq i \leq M+1$ and $1 \leq j \leq N$

$$p_{ij}^X(x,t) = \left\{ \begin{array}{c} \frac{\rho}{2}\left(\frac{\ddot{h}_{ij}^X}{h_{ij}^X} - 2\left(\frac{\dot{h}_{ij}^X}{h_{ij}^X}\right)^2\right)x^2 \\ +\rho\left(\frac{\dot{h}_{ij}^X}{h_{ij}^X}C_{ij}^X - \dot{C}_{ij}^X\right)x \\ +\frac{\rho}{3}\frac{\left|\frac{\dot{h}_{ij}^X}{h_{ij}^X}x - C_{ij}^X\right|^3}{\dot{h}_{ij}^X}f \\ -\frac{\rho}{3}\frac{\left|C_{ij}^X\right|^3}{\dot{h}_{ij}^X}f + p_{ij}^X(0,t) \end{array} \right\}, \tag{17}$$

and for $1 \leq i \leq M$ and $1 \leq j \leq N+1$

$$p_{ij}^Y(y,t) = \left\{ \begin{array}{c} \frac{\rho}{2}\left(\frac{\ddot{h}_{ij}^Y}{h_{ij}^Y} - 2\left(\frac{\dot{h}_{ij}^Y}{h_{ij}^Y}\right)^2\right)y^2 \\ +\rho\left(\frac{\dot{h}_{ij}^Y}{h_{ij}^Y}C_{ij}^Y - \dot{C}_{ij}^Y\right)y \\ +\frac{\rho}{3}\frac{\left|\frac{\dot{h}_{ij}^Y}{h_{ij}^Y}x - C_{ij}^Y\right|^3}{\dot{h}_{ij}^Y}f \\ -\frac{\rho}{3}\frac{\left|C_{ij}^Y(t)\right|^3}{\dot{h}_{ij}^Y}f + p_{ij}^Y(0,t) \end{array} \right\}. \tag{18}$$

The X- and Y- direction fluid forces acting (per unit length) on each rack can be found as follows:

$$F_{ij}^X(t) = \int_{-L_Y/2}^{L_Y/2}\left(p_{ij}^Y(y,t) - p_{ij+1}^Y(y,t)\right)dy,$$

$$F_{ij}^Y(t) = \int_{-L_X/2}^{L_X/2}\left(p_{i+1j}^X(x,t) - p_{ij}^X(x,t)\right)dx,$$

for $1 \leq i \leq M$ and $1 \leq j \leq N$, that is,

$$F_{ij}^X(t) = \left\{ \begin{array}{c} \frac{\rho}{24}\left(\frac{\ddot{h}_{ij}^Y}{h_{ij}^Y} - 2\left(\frac{\dot{h}_{ij}^Y}{h_{ij}^Y}\right)^2\right)L_Y^3 \\ -\frac{\rho}{24}\left(\frac{\ddot{h}_{ij+1}^Y}{h_{ij+1}^Y} - 2\left(\frac{\dot{h}_{ij+1}^Y}{h_{ij+1}^Y}\right)^2\right)L_Y^3 \\ +\frac{\rho}{12}\frac{h_{ij}^Y}{\left(\dot{h}_{ij}^Y\right)^2}\mathcal{T}_{i,j}^Y(t)f \\ -\frac{\rho}{12}\frac{h_{ij+1}^Y}{\left(\dot{h}_{ij+1}^Y\right)^2}\mathcal{T}_{i,j+1}^Y(t)f \\ +\frac{\rho}{3}\left(\frac{\left|C_{ij+1}^Y\right|^3}{\dot{h}_{ij+1}^Y} - \frac{\left|C_{ij}^Y\right|^3}{\dot{h}_{ij}^Y}\right)fL_Y \\ +\left(p_{ij}^Y(0,t) - p_{ij+1}^Y(0,t)\right)L_Y \end{array} \right\}, \tag{19}$$

with $\mathcal{T}_{i,j}^Y(t) =$

$$\left\{ \begin{array}{c} \left|\frac{\dot{h}_{ij}^Y}{h_{ij}^Y}\frac{L_Y}{2} - C_{ij}^Y\right|^3\left(\frac{\dot{h}_{ij}^Y}{h_{ij}^Y}\frac{L_Y}{2} - C_{ij}^Y\right) \\ +\left|\frac{\dot{h}_{ij}^Y}{h_{ij}^Y}\frac{L_Y}{2} + C_{ij}^Y\right|^3\left(\frac{\dot{h}_{ij}^Y}{h_{ij}^Y}\frac{L_Y}{2} + C_{ij}^Y\right) \end{array} \right\}$$

and

$$F_{ij}^Y(t) = \left\{ \begin{array}{c} \frac{\rho}{24}\left(\frac{\ddot{h}_{i+1j}^X}{h_{i+1j}^X} - 2\left(\frac{\dot{h}_{i+1j}^X}{h_{i+1j}^X}\right)^2\right)L_X^3 \\ -\frac{\rho}{24}\left(\frac{\ddot{h}_{ij}^X}{h_{ij}^X} - 2\left(\frac{\dot{h}_{ij}^X}{h_{ij}^X}\right)^2\right)L_X^3 \\ +\frac{\rho}{12}\frac{h_{i+1j}^X}{\left(\dot{h}_{i+1j}^X\right)^2}\mathcal{T}_{i+1,j}^X(t)f \\ -\frac{\rho}{12}\frac{h_{ij}^X}{\left(\dot{h}_{ij}^X\right)^2}\mathcal{T}_{i,j}^X(t)f \\ +\frac{\rho}{3}\left(\frac{\left|C_{ij}^X\right|^3}{\dot{h}_{ij}^X} - \frac{\left|C_{i+1j}^X\right|^3}{\dot{h}_{i+1j}^X}\right)fL_X \\ +\left(p_{i+1j}^X(0,t) - p_{ij}^X(0,t)\right)L_X \end{array} \right\}, \tag{20}$$

with $\mathcal{T}_{i,j}^X(t) =$

$$\left\{ \begin{array}{c} \left|\frac{\dot{h}_{ij}^X}{h_{ij}^X}\frac{L_X}{2} - C_{ij}^X\right|^3\left(\frac{\dot{h}_{ij}^X}{h_{ij}^X}\frac{L_X}{2} - C_{ij}^X\right) \\ +\left|\frac{\dot{h}_{ij}^X}{h_{ij}^X}\frac{L_X}{2} + C_{ij}^X\right|^3\left(\frac{\dot{h}_{ij}^X}{h_{ij}^X}\frac{L_X}{2} + C_{ij}^X\right) \end{array} \right\}.$$

Note that in equations (17)-(20)

$$\ddot{X}_{ij} = \dot{X}_{ij} = 0, \text{ if } i = 0 \text{ or } i = M+1 \text{ and}$$
$$\ddot{Y}_{ij} = \dot{Y}_{ij} = 0, \text{ if } j = 0 \text{ or } j = N+1,$$

as $(X_{ij}(t), Y_{ij}(t))$ are the relative coordinates of each rack.

2.2. Formulation of the coupled system

Assuming that the racks are linear systems with structural mass M_s, damping C_s and stiffness K_s, all these parameters being per unit length, one can deduce the following fluid-structure model:

$$M_\text{s}\ddot{X}_{ij} + C_\text{s}\dot{X}_{ij} + K_\text{s}X_{ij} = F_{ij}^X + F_{ij,\text{aut}}^X, \tag{21}$$

$$M_\text{s}\ddot{Y}_{ij} + C_\text{s}\dot{Y}_{ij} + K_\text{s}Y_{ij} = F_{ij}^Y + F_{ij,\text{aut}}^Y, \tag{22}$$

for $1 \leq i \leq M$ and $1 \leq j \leq N$ where F_{ij}^X, F_{ij}^Y, $F_{ij,\text{aut}}^X$ and $F_{ij,\text{aut}}^Y$ represent, respectively, the above-deduced fluid forces and the external autonomous forces per unit length. Here, the structural parameters have been assumed identical for both directions. However, dealing with asymmetrical systems bring no further difficulties whatsoever.

2.3. Formulation of the complete system

Note that the $2 \times M \times N$ equations (21)-(22) generated by this approach are not sufficient to find all the corresponding unknowns which are summarized in Table 1.

However, between rack or rack/wall positions ij, $ij+1$, $i+1j$ and $i+1j+1$, one can establish the additional equations we need, namely, $(M+1)\times(N+1)-1$ linearly independent equations of compatibility of flow (mass conservation for all nodes but one), $4\times M\times N-(M-1)\times(N-1)$ linearly independent equations of compatibility of pressure (in all corners of each rack except $(M-1)\times(N-1)$ corners) and finally one last equation setting a reference for the pressure.

Unknowns	Number
$X_{ij}(t)$	MN
$Y_{ij}(t)$	MN
$C_{ij}^{X}(t)$	$(M+1)N$
$C_{ij}^{Y}(t)$	$M(N+1)$
$p_{ij}^{X}(0,t)$	$(M+1)N$
$p_{ij}^{Y}(t)$	$M(N+1)$
Total	$6MN+2(M+N)$

Table 1: *Total number of unknowns.*

To complete the model formulation, a number of additional algebraic equations must be stated in order to enforce the flow continuity and pressure compatibility between flow-cells. Here are the compatibility equations of the flow (or continuity in each corner)

$$\left\{\begin{array}{l} \dot{h}_{i+1j+1}^{X}L_X+2C_{i+1j+1}^{X}h_{i+1j+1}^{X} \\ +\dot{h}_{ij+1}^{Y}L_Y+2C_{ij+1}^{Y}h_{ij+1}^{Y} \\ +\dot{h}_{i+1j}^{X}L_X-2C_{i+1j}^{X}h_{i+1j}^{X} \\ +\dot{h}_{i+1j+1}^{Y}L_Y-2C_{i+1j+1}^{Y}h_{i+1j+1}^{Y} \end{array}\right\}=0, \quad (23)$$

where $0\le i\le M$ and $0\le j\le N$. Note that we must disregard one of these equations in order to obtain a set of $(M+1)\times(N+1)-1$ linearly independent equations. In fact, the flow in a corner is completely determined by the flow in the remaining corners.

The equations of compatibility of pressure establish the following $4\times M\times N-(M-1)\times(N-1)$ relations

$$p_{ij}^{X}(-L_X/2,t) = p_{ij}^{Y}(-L_Y/2,t), \quad (24)$$

$$p_{ij}^{X}(L_X/2,t) = p_{ij+1}^{Y}(-L_Y/2,t), \quad (25)$$

$$p_{i+1j}^{X}(-L_X/2,t) = p_{ij}^{Y}(L_Y/2,t), \quad (26)$$

where $1\le i\le M$, $1\le j\le N$ and

$$p_{i+1j}^{X}(L_X/2,t)=p_{i+1j+1}^{Y}(-L_Y/2,t), \quad (27)$$

where $\left\{\begin{array}{c} i=M \\ 1\le j\le N \end{array}\right.$ and $\left\{\begin{array}{c} 1\le i\le M-1 \\ j=N \end{array}\right.$.

Finally

$$\sum_{i=1,j=1}^{i=M+1,j=N} p_{ij}^{X}(0,t)+\sum_{i=1,j=1}^{i=M,j=N+1} p_{ij}^{Y}(0,t)=0, \quad (28)$$

sets a reference for the pressure.

Observe that at the pool walls one has in equations (23)-(27)

$$\ddot{X}_{ij} = \dot{X}_{ij}=0, \text{ if } i=0 \text{ or } i=M+1 \text{ and}$$
$$\ddot{Y}_{ij} = \dot{Y}_{ij}=0, \text{ if } j=0 \text{ or } j=N+1,$$

whenever In Table 2 we summarize the abovementioned equations defining our linearized model for the fluid-coupled vibratory responses of the system.

Equation	Number of Equations
(21)	MN
(22)	MN
(23)	$(M+1)(N+1)-1$
(24)-(27)	$4MN-(M-1)(N-1)$
(28)	1
Total	$6MN+2(M+N)$

Table 2: *Equations of the nonlinear model for the fluid-coupled vibratory response of the system.*

All these equations represent a set of differential-algebraic equations (DAE's). That is, among those equations, some of them are pure algebraic constrains between unknowns. Clearly, this is the case of equation (28). Note that this class of equations arise naturally in many applications but present numerical and analytical difficulties which do not occur with systems of ordinary differential equations Brenan et al (1996). In our case the DAE's developed can be classified as a nonlinear differential-algebraic system of equations

Note that these equations can be written and established for generic systems of $M\times N$ racks entirely on a symbolic computer environment as it was done here for the ilustrative computations.

3. NUMERICAL SIMULATIONS

Define the set of differential-algebraic equations corresponding to our model as

$$\mathbf{F}(\dot{\mathbf{v}},\mathbf{v},t)=0 \quad (29)$$

where $\mathbf{v}$ is the vector of unknowns. The simplest first order backward difference formula is the implicit

Euler method

$$\mathbf{F}\left(\frac{\mathbf{v}_{n+1}-\mathbf{v}_n}{t_{n+1}-t_n},\mathbf{v}_{n+1},t_{n+1}\right)=0 \qquad (30)$$

in which equation (29) is approximated by finite differences [Brenan et al (1996)]. In the present work we used a fourth and fifth-order generalization of (30) coded in MATLAB [Roberts (1998)].

In order to validate our nonlinear model, several numerical simulations were performed over fuel pools with one centered single rack and fuel pools with six racks regularly stored in 2 lines and 3 columns. The present numerical simulations agreed with our previous work, for low vibration amplitudes (with respect to the average gaps), when the linearization assumptions were fulfilled [Moreira and Antunes (2002)]. However when nonlinear flow effects are significant, our new nonlinear model yields much more realistic predictions. Consider two fuel pools (Pool A and Pool B), using dissimilar fluid gaps, each one with six racks regularly stored in 2 lines and 3 columns. Their response to the same seismic excitation is presented next. The seismic excitation used was the east-west component of the Loma Prieta earthquake in October, 1989, applied along the X-direction (also an axis of symmetry of the storage pools with the racks).

	Pool A	Pool B
L_X (m)	2	2
L_Y (m)	2	2
H_i^X	0.2	0.03
H_j^Y	0.2	0.03

Table 3: *Main geometrical parameters for the numerical simulations.*

All numerical simulations were performed with the main geometrical, physical and structural modal parameters presented in Tables 3 and 4. The time-step used $\triangle t = 0.005$, was one order of magnitude smaller than $1/(2f_{\max})$, with $f_{\max} \approx 20$ Hz (maximum frequency of interest assuming a dominant frequency in the seismic spectrum below 10 Hz). In order to provide an appropriate spectral resolution these numerical simulations were performed over an interval of 35 s.

4. RESULTS AND DISCUSSION

In Figures 2 and 3 we display the spectral response in both directions of the rack in position $(1,1)$ when all the fuel storage pools were submitted to the Loma Prieta earthquake applied along the X-direction. Note that in Pool A the inter-rack gaps and wall/rack gaps are 0.2 m, while in Pool B are only 0.03 m, so that nonlinear squeeze-film and dissipative effects are enhanced.

Structural mass, M_s (kg)	32000
Structural damping, C_s (N s/m)	8000
Structural stiffness, K_s (N/m)	5×10^6
Modal frequency in air, f_s (Hz)	2
Reduced damping in air, ζ	0.01
Rack density, $(\rho_s/\rho_{\text{water}})$	8
fricton factor, f	0.01

Table 4: *Physical and structural modal parameters for the numerical simulations.*

In spite of the excitation being the same on each rack and only along the direction X responses displayed in Figures 2 and 3 exhibit motions perpendicular to this direction. This is accounted for the presence of a strong fluid-structure interaction, which coupleds all racks and the two motions directions.

In Figure 2 one can observe the spectra response concentrated around 1.5 Hz. Note that the in air, the modal frequency of the structure was 2 Hz. This difference is obviously due to the fluid added mass effect.

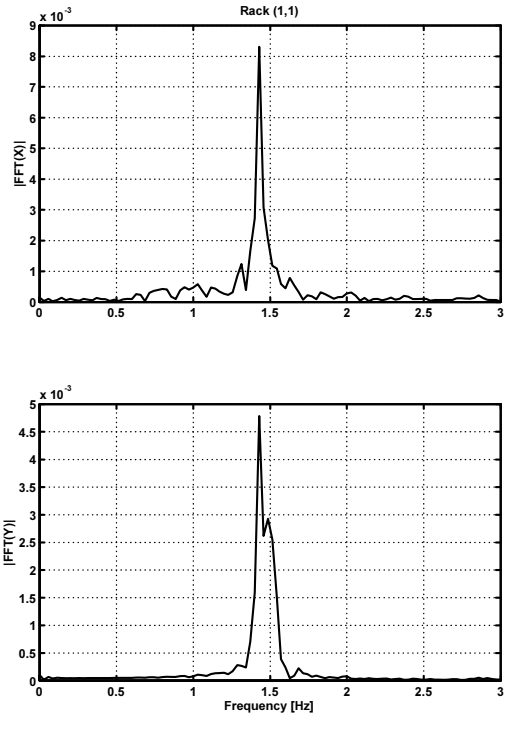

Figure 2: *Pool A. Spectral response of rack* $(1,1)$ *to the seismic excitation applied along direction* X*: (a) responses along direction* X *and (b) responses along direction* Y.

In Figure 3 the spectral response energy of rack $(1,1)$, in both directions, is now diluted over a larger frequency interval (between 0.4 Hz and 1.4 Hz). This energy spread is related to the nonlinear flow forces, as a result of the smaller inter-rack and rack/wall gaps, which enhanced the squeeze-film and dissipative effects. Additionally one observe also that the increased fluid added mass lowered even further the response frequencies of our system.

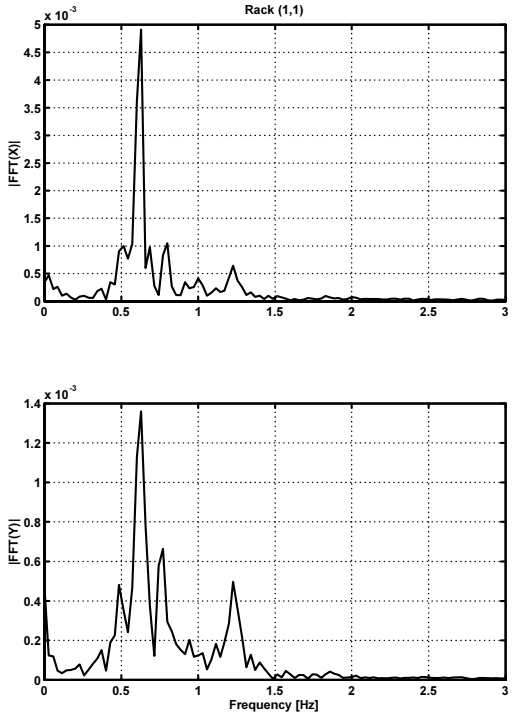

Figure 3: *Pool B. Spectral response of rack* $(1,1)$ *to the seismic excitation applied along direction* X*: (a) responses along direction* X *and (b) responses along direction* Y*.*

5. CONCLUSIONS

In this paper, we propose a generalization of our previous linearized approach [Moreira and Antunes (2002)], introducing a nonlinear model for the fluid-coupled vibratory responses of nuclear fuel racks, neglecting three-dimensional flow effects and assuming small gaps between the fuel assemblies. The proposed methodology can be automatically implemented on a symbolic computer environment. Numerical simulations highlighted the significance of nonlinear flow effects at high vibration amplitudes (or small inter-rack and wall/rack gaps). Under such conditions, the proposed approach yields more realistic predictions than our previous work.

6. REFERENCES

Antunes, J. and Piteau, P., 2001, A Nonlinear Model for Squeeze-film Dynamics Under Axial Flow, Proceedings of the ASME Pressure Vessel and Piping Conference, Atlanta, USA, July 2001, **420-2**: 53-62.

Blevins, R., 1984, Fluid Dynamics, Van Nostrand Reinhold Company, New York.

Brenan, K. E., Campbell, S. L. and Pezold, L. R., 1996, Numerical Solution of Initial-Value Problems in Differential-Algebraic Equations, SIAM.

Broc, D., Queval J and Chaudat, T, 2000, Fluid Structure Interaction For Nuclear Spent Fuel racks, Proceedings of PVP , Emerging Technologies in Fluids, Structures and Fluid/Structure Interactions. Pressure Vessel and Piping Conference, Seattle, USA, July 2000, PVP **414-2**: 171-177.

Hinderks, M., Ungoreit, H. and Kremer, G., 2001, Improved method to demonstrate the structural integrity of high density fuel storage racks. *Nuclear Engineering and Design* **206**: 177-184.

Hindmarsh, A. C. and Petzold, L. R., 1988, Numerical Methods for Solving Ordinary Differential Equations and Differential/Algebraic Equations, Energy Tech. Rev., September, 23-36, 1988.

Hirs, G., 1973, A Bulk Flow Theory for Turbulence in Lubrificant Films, *ASME Journal of Lubrification Technology*, **95**: 137-146.

Moreira, M. and Antunes, J., 2002, A simplified Linearized Model for the fluid-coupled vibrations of spent nuclear fuel racks. *Journal of Fluids and Structures* **16**(7): 971-987.

Roberts, A. J., 1998, *Differential - Algebraic equations solver DAE*, http://www.mathworks.com /support /ftp /diffeqv5.shtml.

Stabel, J. and Ren, M., 2001, Fluid-structure-interaction for the analysis of the dynamics of fuel storage racks in the case of seismic loads. *Nuclear Engineering and Design* **206**: 167:176.

Zhao, Y., Wilson, P. R. and Stevenson, 1996, Nonlinear 3-D dynamic time history in the reracking modifications for a nuclear power plant. *Nuclear Engineering and Design* **165**: 199-211.